

# Highly Confined Hybrid Plasmonic Modes Guided by Nanowire-Embedded-Metal Grooves for Low-Loss Propagation at 1550 nm

Yusheng Bian<sup>1</sup>, Zheng Zheng<sup>1</sup>, Xin Zhao, Yalin Su, Lei Liu, Jiansheng Liu, Jinsong Zhu, and Tao Zhou

**ABSTRACT**—A waveguiding configuration consisting of a semiconductor nanowire embedded in a dielectric-coated V-shaped metal groove is presented. The modal properties of the fundamental quasi-TE hybrid plasmonic mode are investigated at the wavelength of 1550 nm. Simulation results reveal that by tuning the size of the nanowire, the hybridization between the dielectric mode, and plasmonic mode could be effectively controlled. Through appropriate design, the hybrid mode could be strongly localized in the nanowire and the gap regions on each side, featuring both tight-mode confinement and low propagation loss. Besides, the compromise between confinement and loss could also be balanced by controlling the angle or depth of the metal groove. Moreover, it is found that the hybrid mode could exist for a wide geometrical parameter range, even when the corresponding metal groove by itself does not support a guided channel plasmon polariton mode. The proposed hybrid structure is technologically simple and compatible with planar fabrication methods while avoiding alignment errors.

**INDEX TERMS**—Optical waveguides, optical planar waveguides, plasmons.

## I. INTRODUCTION

**S**URFACE plasmon polariton (SPP) structures combining the size of nanoelectronics and the speed of microphotonics are proposed as a promising solution for the next generation, highly integrated photonic components and circuits [1]. Although a wide range of SPP-based waveguides and components have been theoretically proposed, a less number of them have been experimentally demonstrated because of the huge

loss caused by the metallic structure and the stringent practical fabrication requirements [2]. The long-range SPP (LR-SPP) waveguides are among one of the few candidates so far that have demonstrated the realization of complex photonic components and on-chip integrations [3], [4], mainly due to their ultralow propagation loss. However, their rather weak confinement with mode size comparable to that of the conventional low-index contrast dielectric waveguides renders great challenges for large-scale integrations. One of the promising candidate for efficient guiding and confining SPP waves at the subwavelength scale with relatively low propagation loss is the channel plasmon polariton (CPP) waveguides in the form of a V-shaped or U-shaped channel milled on a metallic substrate [5]–[10]. CPP waveguides could balance the tradeoff between the propagation loss and mode confinement to a certain extent. The subwavelength field confinement has enabled the realization of various integrated photonic components, including Y-splitters, Mach-Zehnder interferometers, waveguide-ring resonators, add-drop multiplexers, and Bragg gratings [11], [12]. Another attractive advantage of the CPP waveguides and components is their compatibility with standard planar fabrication techniques (e.g., using the focused-ion beam (FIB) milling [11] or combined UV and nanoimprint lithography methods [13]). In contrast to other SPP counterparts that may require relatively strict fabrication condition and complicated fabrication procedures, CPP waveguides are relatively simple to make [11] and also offer compatibility with mass production [13], hence making them promising candidates for various applications.

On the other hand, recent advancement in novel plasmonic waveguiding configurations has led to the proposal and demonstration of a host of hybrid plasmonic structures [14]–[28], which combine the advantages of both semiconductor and plasmonic waveguides and enable light transmission in the deep subwavelength, low-index gap, promising to achieve long-range propagation with tight-mode confinement. Various types of active and passive plasmonic devices including nanolasers, couplers, splitters, and ring resonators have also been theoretically studied and experimentally demonstrated [29]–[36]. The characteristics of the hybrid mode can be shifted from dielectric-waveguide-mode-like toward SPP-like through tuning the hybridization between the SPP modes and the waveguide modes [14]. As the properties of the hybrid plasmonic modes are heavily influenced by those of the corresponding uncoupled SPP modes, employing a different metal nanostructure may result in dramatically modified modal behavior. However, the steps to

Manuscript received May 27, 2012; revised July 24, 2012; accepted August 1, 2012. This work was supported by the 973 Program under Grant 2009CB930701, the National Science Foundation of China under Grant 60921001/61077064, the Program for Changjiang Scholars and Innovative Research Team in University PCSIRT, State Education Ministry (SEM), National key scientific instruments and equipment development special fund management under Grant 2011YQ0301240502, and the Innovation Foundation of Beihang University for Ph.D. Graduates.

Y. Bian, Z. Zheng, X. Zhao, Y. Su, L. Liu, and J. Liu are with the School of Electronic and Information Engineering, Beihang University, Beijing 100191, China (e-mail: bianys@126.com; zhengzheng@buaa.edu.cn; zhaoxin127@163.com; ylsu@ee.buaa.edu.cn; liuleiatbest@163.com).

J. Zhu is with the National Center for Nanoscience and Technology, Beijing 100190, China (e-mail: jizhu88@gmail.com).

T. Zhou is with the Department of Physics, New Jersey Institute of Technology, Newark, NJ 07102 USA (e-mail: taozhou@njit.edu).

Color versions of one or more of the figures in this paper are available online at <http://ieeexplore.ieee.org>.

Digital Object Identifier 10.1109/JSTQE.2012.2212002

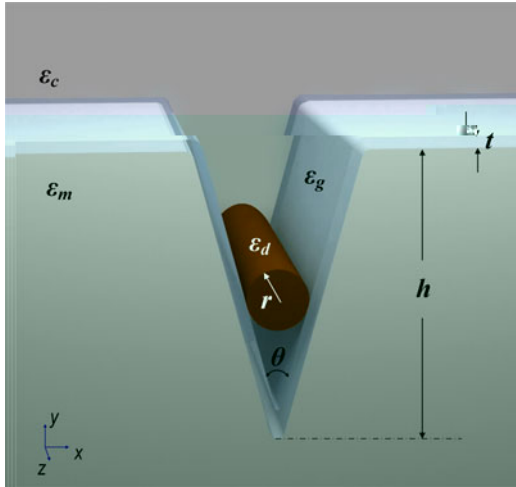


Fig. 1. Geometry of the hybrid metal groove waveguide.

fabricate complicated metallic nanostructures result in an extra complexity. Besides, for some of the hybrid structures, the accurate alignment between different layers or patterns could be challenging [15], [30], [37], and the fabrication errors may adversely affect the guiding capability of the hybrid modes.

In this paper, we propose a novel hybrid plasmonic waveguide by integrating high-index semiconductor nanowires with dielectric-coated metal groove plasmonic structures (also can be named as dielectric-loaded groove waveguides [38]–[40]). Through combining the strong mode confinement capability of the CPP waveguide with the hybrid concept, the formed hybrid plasmonic structure provides a new avenue to support highly efficient hybrid plasmonic modes, which feature both strong mode confinement and low-propagation loss at the telecom wavelength. The proposed straight-type waveguide could be fabricated using planar techniques. Similar to conventional CPP waveguides, the FIB method could be used to create the metal groove and the semiconductor nanowire is then placed inside the groove after a thin dielectric layer is coated on the metallic surface. Compared to many other plasmonic structures, fewer fabrication steps are needed and it is alignment-free, alleviating some of the undesirable fabrication imperfections. More complex passive photonic components based on such a waveguide may also be realized by employing micromanipulation process, which had been widely used to build versatile nanowire-based devices such as branch- [41] and loop-type structures [42] without damaging the nanowires.

## II. GEOMETRY AND MODAL PROPERTIES OF THE PROPOSED HYBRID GROOVE WAVEGUIDES

The proposed hybrid metal groove waveguide shown in Fig. 1 consists of a high-index dielectric nanowire separated from a V-shaped metallic substrate by a nanometer-scale-thick low dielectric constant gap. Here, the nanowire is assumed to be embedded inside the groove and supported in direct contact by the homogeneous low-index dielectric coating layer. The radius of the nanowire is  $r$ . The metal groove has a tip angle of  $\theta$  and a depth of  $h$ . The thickness of the low-index dielectric coating

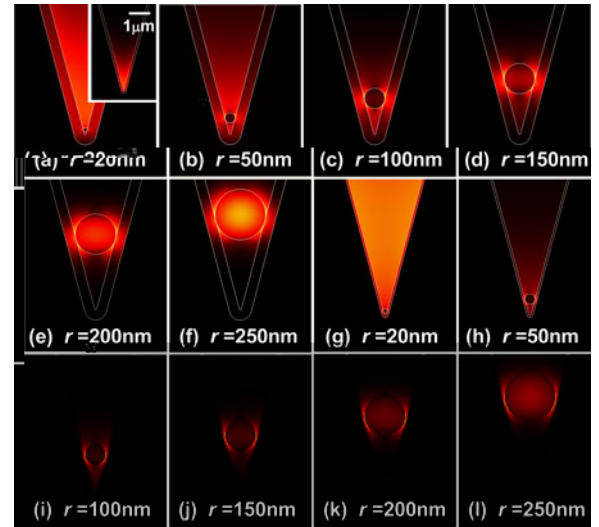


Fig. 2.  $|E|^2$  distributions of the fundamental quasi-TE plasmonic mode of hybrid V-groove waveguides with different GaAs nanowires: (a)–(f)  $r = 30, 50, 100, 150, 200, 250$  nm, (g)–(l)  $r = 20, 50, 100, 150, 200, 250$  nm.

layer is  $t$ . All the corners in the waveguiding structure are considered as rounded of a fixed 10-nm curvature radius for the inner corners, while the outer corners have a curvature radius of  $(10 + r)$  nm to keep a constant gap width. The modal characteristics of the hybrid metal groove waveguides are investigated at  $\lambda = 1550$  nm. The metallic substrate is assumed to be silver (Ag), the high-index dielectric is GaAs, and the low-index dielectric gap layer is silica ( $\text{SiO}_2$ ) with air as the cladding. The permittivities of air,  $\text{SiO}_2$ , GaAs, and Ag are  $\epsilon_c = 1$ ,  $\epsilon_m = 2.25$ ,  $\epsilon_d = 12.25$ , and  $\epsilon_g = 129 + 3.3j$  [43], respectively. The modal properties are investigated by means of the finite-element method using COMSOL. The eigenmode solver is used with the scattering boundary condition, which is a commonly employed approach to mimic the necessary open boundary [14]. Convergence tests are done to ensure that the numerical boundaries and meshing do not interfere with the solutions.

The waveguide configuration firstly considered here, has a deep enough metal groove (sufficiently large to avoid the edge effects) with a tip angle of  $30^\circ$ , to ensure that the structure without the GaAs nanowire could support bound CPP modes [5], [9], [44]. In such a case, as the fundamental hybrid plasmonic mode results from the coupling between the CPP mode and the dielectric mode, and is denoted as the hybrid CPP mode. We note that the dielectric mode could also be coupled with higher order CPP modes under certain geometries, but here we will only focus our discussions on the properties of the fundamental hybrid CPP mode. Simulation results of the electric field for the fundamental quasi-TE hybrid mode with different geometries are shown in Fig. 2. For configurations with a relatively thicker  $\text{SiO}_2$  layer (e.g.,  $t = 100$  nm), increasing the GaAs nanowire radius from 20 to 250 nm results in an evolution of the hybrid mode behavior from CPP-like to dielectric-like. When the nanowire is small ( $r = 20$  nm), the field is mainly guided at the bottom of the metal groove [see the inset of Fig. 2(a)] similar as conventional CPP waveguides. As the nanowire gets larger, the mode field

begins shifting toward where the nanowire sits (e.g., 50 nm). A further increase in the size of the nanowire results in more field concentrated in both the nanowire and the adjacent gap layer (e.g., 100, 150 nm), corresponding to the strongest coupling between the CPP and dielectric mode. Finally, almost all of the energy could be stored inside the nanowire when reaches certain values (e.g., 200 and 250 nm), where the corresponding mode loss is very low. While for the case of a thin silica layer (e.g., 20 nm), the trend of the mode behavior with various nanowires is almost the same as that of the thick layer. The only difference is that when the nanowire is relatively large, the hybrid mode no longer displays either dielectric- or CPP-like properties, but gets strongly confined in the low-index gap, as clearly seen in Fig. 2(j) (l). Simulation also illustrates that further reduction of the thickness of the SiO<sub>2</sub> layer (e.g., 10 nm) would result in more pronounced field enhancement in the gap and smaller mode area, indicating tighter mode confinement could be achieved. Besides, for all the studied cases, when the nanowire is rather large, the quasi-TM mode could also be supported by the structure, which has dielectric-like modal properties with relatively low-propagation loss due to the less overlap of the mode profile with the metal sidewalls.

The modal properties including the modal effective index  $N_{\text{eff}}$ , propagation length  $L_p$ , and normalized mode area ( $A_{\text{eff}}/A_0$ ) of the fundamental hybrid plasmonic mode of our proposed structures with different GaAs nanowires and SiO<sub>2</sub> layers are shown in Fig. 3 as  $r$  varies from 20 to 250 nm. The propagation length is given by  $L_p = \lambda/[4\pi \text{Im}(\beta)]$ .  $A_0$  is the diffraction-limited mode area in free space and defined as  $\lambda^2/4$ . The effective mode area  $A_{\text{eff}}$  is calculated using

$$\left( \iint W(r) \right)^2 / \left( \iint W(r)^2 \right) \quad (1)$$

where the electromagnetic energy density  $W$  is defined the same as in [14], [45], [46]. Fig. 3(a) illustrates that  $N_{\text{eff}}$  increases monotonically when  $r$  gets bigger. Such a trend gets more pronounced for relatively large GaAs nanowire with thinner SiO<sub>2</sub> layer, due to the stronger interaction between the plasmonic and dielectric mode, while the propagation length and mode area are shown to decrease first before they increase with increased  $r$ . Extended propagation length and, correspondingly, larger mode area are observed when the GaAs nanowire is either very small or very large. When the GaAs nanowire has a moderate size, strong coupling between the CPP mode and dielectric mode occurs, where relatively short propagation length with small mode area is expected. Under such conditions, between 30% and 40% of the total power could be squeezed into the gaps on both sides of the GaAs nanowire, indicating tighter mode confinement achieved in the low-index gap region than the conventional hybrid plasmonic waveguide [14]. While on the other hand a substantial portion of the total power could also be stored in the high-index GaAs nanowire, and such power ratio could be further increased, even up to nearly 90% (e.g., 250 nm), by employing a larger nanowire, which is also higher than the corresponding conventional hybrid waveguide on metal substrate. Such property may facilitate sufficient

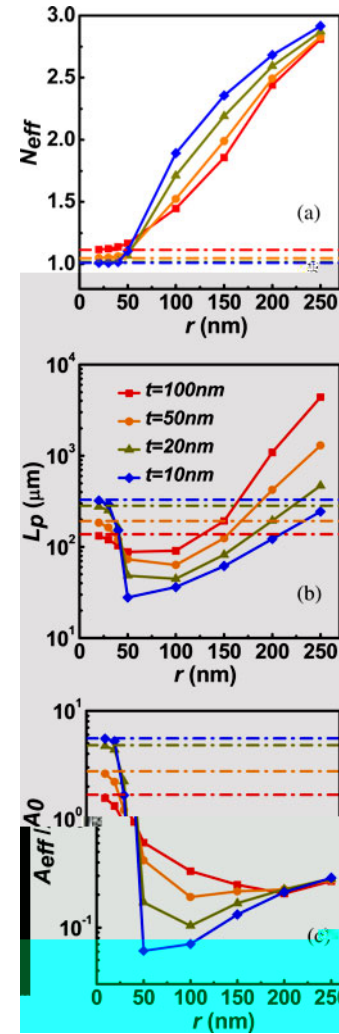


Fig. 3. Dependence of the modal properties of the fundamental hybrid CPP mode on the radius of the GaAs nanowire. (a) Modal effective index  $N_{\text{eff}}$ . (b) Propagation length  $L_p$ . (c) Normalized mode area  $A_{\text{eff}}/A_0$ . Dash-dotted lines correspond to the CPP modes supported by the metal grooves with different SiO<sub>2</sub> coating layers.

modal overlap with the gain medium, beneficial for possible applications like nanolasers [29], [33]. As also seen in Fig. 3(b) and (c), for the considered range of geometry parameters, sub-wavelength mode confinement could be achieved along with relatively long-range propagation distance (around tens to hundreds of microns), indicating nice guiding properties of the fundamental hybrid CPP mode.

The effects of metallic groove angle and groove depth on modal properties are then investigated. Fig. 4 shows the calculated results of the  $L_p$  and  $A_{\text{eff}}/A_0$  with different  $\theta$  and  $d$ . It is illustrated that the waveguide with a deep metal groove has lower propagation loss with a sharper  $\beta$ , at the cost of a larger mode area. Furthermore, for relatively large  $d$  (e.g.,  $>1 \mu\text{m}$  for  $\theta = 16^\circ$ ), the modal properties of the quasi-TE hybrid mode quickly reach those under infinitely large  $d$ , indicating robust waveguiding characteristics against the variation of the metal groove when the groove is not too shallow. On the other hand, when  $d$  is very small, the hybridization between the dielectric nanowire mode and the SPP along the top edges becomes

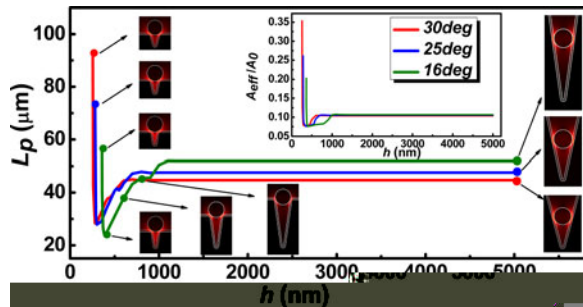


Fig. 4. Propagation length  $L_p$  of the studied hybrid plasmonic mode supported by the waveguide with different  $\theta$  and  $h$  ( $h = 100$  nm,  $h = 20$  nm), where the inset shows the corresponding normalized mode area ( $A_{\text{eff}}/A_0$ ) and the electric field distributions for different waveguiding structures.

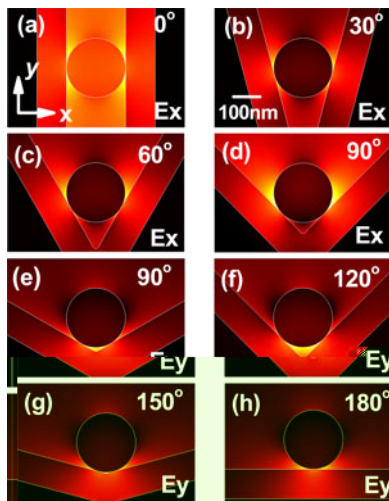


Fig. 5. Field distributions of the dominant electric component when  $\theta$  changes from  $0^\circ$  to  $180^\circ$ :  $E_x$  for the quasi-TE mode and  $E_y$  for the quasi-TM mode. ( $h = 100$  nm).

more pronounced, resulting in more field localized in the metal structure, and thus increased the propagation loss. Further reduction of the groove depth causes the mode shifted toward cutoff, where the effective index of the mode approaches that of the air cladding's, with dramatically reduced propagation loss and increased mode area (also see the field distributions in the inset).

Simulations also demonstrate that hybrid modes could be supported by the proposed waveguide configuration with a much larger range of groove angles, even when the corresponding metal structure does not support guided CPP modes. Here, the electric field distributions of the fundamental hybrid modes are shown in Fig. 5 with groove angle increasing from  $0^\circ$  to  $180^\circ$ , where the extreme case of  $0^\circ$  corresponds to a hybrid plasmonic structure with a nanowire placed between two parallel vertical metal walls separated by  $\text{SiO}_2$  buffer layers. Similar configurations, which can be called hybrid metal insulator metal waveguides, have been investigated both theoretically and experimentally in previous study [37], [47] [51]. On the other hand, when the angle reaches  $180^\circ$ , the structure turns into a conventional hybrid plasmonic waveguide with a flat metallic substrate. Fig. 5 illustrates that when  $\theta$  is small (e.g.,  $\ll 90^\circ$ ), the

hybrid mode is quasi-TE-like with  $E_x$  as the dominant electric component. On the other hand, for large angles (e.g.,  $>90^\circ$ ), the fundamental mode exhibits a quasi-TM-like behavior. Here, as the metal groove structure may not support a CPP mode with large tip angles, the hybrid mode might be better named as a hybrid trench mode instead of a hybrid CPP mode. At certain critical angles (e.g.,  $90^\circ$ ), the hybrid groove waveguide could support both quasi-TE and quasi-TM hybrid plasmonic modes. The aforementioned results illustrate that when  $\theta$  varies within the range of  $0^\circ$  to  $180^\circ$ , the fundamental hybrid mode undergoes a polarization change, indicating a transformation of hybrid TE mode to hybrid TM mode. On the other hand, for more realistic configurations with a finite groove depth and a sharp angle (supporting hybrid quasi-TE mode), polarization rotation could also be realized by continuously decreasing the groove depth.

Recent work has demonstrated that in contrast to the conventional CPP waveguides, realis-

- [8] E. Moreno, F. J. Garcia-Vidal, S. G. Rodrigo, L. Martin-Moreno, and S. I. Bozhevolnyi, Channel plasmon-polaritons: Modal shape, dispersion, and losses, *Opt. Express*, vol. 31, pp. 3447–3449, 2006.
- [9] S. I. Bozhevolnyi, Effective-index modeling of channel plasmon polaritons, *Opt. Express*, vol. 14, pp. 9467–9476, Oct. 2006.
- [10] M. Yan and M. Qiu, Guided plasmon polariton at 2-D metal corners, *Opt. Express*, vol. 24, pp. 2333–2342, 2007.
- [11] S. I. Bozhevolnyi, V. S. Volkov, E. Devaux, J. Y. Laluet, and T. W. Ebbesen, Channel plasmon subwavelength waveguide components including interferometers and ring resonators, *Nature*, vol. 440, pp. 508–511, 2006.
- [12] V. S. Volkov, S. I. Bozhevolnyi, E. Devaux, J. Y. Laluet, and T. W. Ebbesen, Wavelength selective nanophotonic components utilizing channel plasmon polaritons, *Opt. Express*, vol. 7, pp. 880–884, 2007.
- [13] R. B. Nielsen, I. Fernandez-Cuesta, A. Boltasseva, V. S. Volkov, S. I. Bozhevolnyi, A. Klukowska, and A. Kristensen, Channel plasmon polariton propagation in nanoimprinted V-groove waveguides, *Opt. Express*, vol. 33, pp. 2800–2802, 2008.
- [14] R. F. Oulton, V. J. Sorger, D. A. Genov, D. F. P. Pile, and X. Zhang, A hybrid plasmonic waveguide for subwavelength confinement and long-range propagation, *Nature Photonics*, vol. 2, pp. 496–500, 2008.
- [15] D. X. Dai and S. L. He, A silicon-based hybrid plasmonic waveguide with a metal cap for a nano-scale light confinement, *Opt. Express*, vol. 17, pp. 16646–16653, Sep. 2009.
- [16] Y. S. Bian, Z. Zheng, X. Zhao, J. S. Zhu, and T. Zhou, Symmetric hybrid surface plasmon polariton waveguides for 3D photonic integration, *Opt. Express*, vol. 17, pp. 21320–21325, 2009.
- [17] I. Avrutsky, R. Soref, and W. Buchwald, Sub-wavelength plasmonic modes in a conductor-gap-dielectric system with a nanoscale gap, *Opt. Express*, vol. 18, pp. 348–363, 2010.
- [18] M. Z. Alam, J. Meier, J. S. Aitchison, and M. Mojahedi, Propagation characteristics of hybrid modes supported by metal-low-high index waveguides and bends, *Opt. Express*, vol. 18, pp. 12971–12979, Jun. 2010.
- [19] Y. S. Bian, Z. Zheng, Y. Liu, J. S. Zhu, and T. Zhou, Dielectric-loaded surface plasmon polariton waveguide with a holey ridge for propagation-loss reduction and subwavelength mode confinement, *Opt. Express*, vol. 18, pp. 23756–23762, 2010.
- [20] D. Chen, Cylindrical hybrid plasmonic waveguide for subwavelength confinement of light, *Opt. Express*, vol. 49, pp. 6868–6871, Dec. 2010.
- [21] V. J. Sorger, Z. Ye, R. F. Oulton, Y. Wang, G. Bartal, X. Yin, and X. Zhang, Experimental demonstration of low-loss optical waveguiding at deep sub-wavelength scales, *Opt. Express*, vol. 2, pp. 331–335, 2011.
- [22] Y. S. Bian, Z. Zheng, Y. Liu, J. S. Zhu, and T. Zhou, Hybrid wedge plasmon polariton waveguide with good fabrication-error-tolerance for ultra-deep-subwavelength mode confinement, *Opt. Express*, vol. 19, pp. 22417–22422, 2011.
- [23] Y. Su, Z. Zheng, Y. Bian, Y. Liu, J. Liu, J. Zhu, and T. Zhou, Low-loss silicon-based hybrid plasmonic waveguide with an air nanotrench for sub-wavelength mode confinement, *Opt. Express*, vol. 6, pp. 643–645, Aug. 2011.
- [24] C. C. Huang, Hybrid plasmonic waveguide comprising a semiconductor nanowire and metal ridge for low-loss propagation and nanoscale confinement, *Opt. Express*, vol. 18, no. 6, pp. 1661–1668.
- [25] L. Chen, X. Li, G. P. Wang, W. Li, S. H. Chen, L. Xiao, and D. S. Gao, A Silicon-based 3-D hybrid long-range plasmonic waveguide for nanophotonic integration, *Opt. Express*, vol. 30, pp. 163–168, Jan. 2012.
- [26] C.-L. Zou, F.-W. Sun, C.-H. Dong, Y.-F. Xiao, X.-F. Ren, L. Lv, X.-D. Chen, J.-M. Cui, Z.-F. Han, and G.-C. Guo, Movable ber-integrated hybrid plasmonic waveguide on metal film, *Opt. Express*, vol. 24, no. 6, pp. 434–436, Mar. 2012.
- [27] M. Fujii, J. Leuthold, and W. Freude, Dispersion relation and loss of sub-wavelength confined mode of metal-dielectric-gap optical waveguides, *Opt. Express*, vol. 21, no. 6, pp. 362–364, Mar. 2009.
- [28] Y. S. Bian, Z. Zheng, X. Zhao, Y. L. Su, L. Liu, J. S. Liu, J. S. Zhu, and T. Zhou, Guiding of long-range hybrid plasmon polariton in a coupled nanowire array at deep-subwavelength scale, *Opt. Express*, vol. 24, no. 15, pp. 1279–1281, 2012.
- [29] R. F. Oulton, V. J. Sorger, T. Zentgraf, R. M. Ma, C. Gladden, L. Dai, G. Bartal, and X. Zhang, Plasmon lasers at deep subwavelength scale, *Nature*, vol. 461, pp. 629–632, Oct. 2009.
- [30] M. Wu, Z. H. Han, and V. Van, Conductor-gap-silicon plasmonic waveguides and passive components at subwavelength scale, *Opt. Express*, vol. 18, pp. 11728–11736, May 2010.
- [31] H. S. Chu, E. P. Li, P. Bai, and R. Hegde, Optical performance of single-mode hybrid dielectric-loaded plasmonic waveguide-based components, *Opt. Express*, vol. 96, pp. 221103-1–221103-3, 2010.
- [32] X. Y. Zhang, A. Hu, J. Z. Wen, T. Zhang, X. J. Xue, Y. Zhou, and W. W. Duley, Numerical analysis of deep sub-wavelength integrated plasmonic devices based on semiconductor-insulator-metal strip waveguides, *Opt. Express*, vol. 18, pp. 18945–18959, 2010.
- [33] Y. S. Bian, Z. Zheng, Y. Liu, J. S. Zhu, and T. Zhou, Coplanar plasmonic nanolasers based on edge-coupled hybrid plasmonic waveguides, *Opt. Express*, vol. 23, no. 13, pp. 884–886, 2011.
- [34] H. S. Chu, E. P. Li, P. Bai, and R. Hegde, Hybrid dielectric-loaded plasmonic waveguide-based power splitter and ring resonator: Compact size and high optical performance for nanophotonic circuits, *Opt. Express*, vol. 6, pp. 591–597, Dec. 2011.
- [35] J. Tian, Z. Ma, Q. A. Li, Y. Song, Z. H. Liu, Q. Yang, C. L. Zha, J. Akerman, L. M. Tong, and M. Qiu, Nanowaveguides and couplers based on hybrid plasmonic modes, *Opt. Express*, vol. 97, pp. 231121-1–231121-3, Dec. 2010.
- [36] C. Horvath, D. Bachman, M. Wu, D. Perron, and V. Van, Polymer hybrid plasmonic waveguides and microring resonators, *Opt. Express*, vol. 23, no. 17, pp. 1267–1269, Sep. 2011.
- [37] M. S. Kwon, Metal-insulator-silicon-insulator-metal waveguides compatible with standard CMOS technology, *Opt. Express*, vol. 19, pp. 8379–8393, Apr. 2011.
- [38] B. Steinberger, A. Hohenau, H. Ditlbacher, A. L. Stepanov, A. Drezet, F. R. Aussenegg, A. Leitner, and J. R. Krenn, Dielectric stripes on gold as surface plasmon waveguides, *Opt. Express*, vol. 88, pp. 094104-1–094104-3, Feb. 2006.
- [39] T. Holmgaard, Z. Chen, S. I. Bozhevolnyi, L. Markey, A. Dereux, A. V. Krasavin, and A. V. Zayats, Wavelength selection by dielectric-loaded plasmonic components, *Opt. Express*, vol. 94, pp. 051111-1–051111-3, 2009.
- [40] T. Holmgaard, J. Gosciniaik, and S. I. Bozhevolnyi, Long-range dielectric-loaded surface plasmon-polariton waveguides, *Opt. Express*, vol. 18, pp. 23009–23015, 2011.
- [41] H. Wei, Z. Wang, X. Tian, M. Kall, and H. Xu, Cascaded logic gates in nanophotonic plasmon networks, *Opt. Express*, vol. 2, pp. 387–391, Jul. 2011.
- [42] Y. Xiao, C. Meng, P. Wang, Y. Ye, H. Yu, S. Wang, F. Gu, L. Dai, and L. Tong, Single-nanowire single-mode laser, *Opt. Express*, vol. 11, pp. 1122–1126, Mar. 2011.
- [43] P. B. Johnson and R. W. Christy, Optical constants of the noble metals, *Phys. Rev.*, vol. 6, pp. 4370–4379, 1972.
- [44] S. Lee and S. Kim, Long-range channel plasmon polaritons in thin metal film V-grooves, *Opt. Express*, vol. 19, pp. 9836–9847, May 2011.
- [45] J. A. Dionne, L. A. Sweatlock, H. A. Atwater, and A. Polman, Plasmon slot waveguides: Towards chip-scale propagation with subwavelength-scale localization, *Opt. Express*, vol. 73, pp. 035407-1–035407-9, 2006.
- [46] R. F. Oulton, G. Bartal, D. F. P. Pile, and X. Zhang, Confinement and propagation characteristics of subwavelength plasmonic modes, *Opt. Express*, vol. 10, pp. 105018-1–105018-14, 2008.
- [47] N. N. Feng, M. L. Brongersma, and L. Dal Negro, Metal-dielectric slot-waveguide structures for the propagation of surface plasmon polaritons at 1.55  $\mu\text{m}$ , *Opt. Express*, vol. 43, no. 6, pp. 479–485, 2007.
- [48] D. X. Dai and S. L. He, Low-loss hybrid plasmonic waveguide with double low-index nano-slots, *Opt. Express*, vol. 18, pp. 17958–17966, 2010.
- [49] J. T. Kim, CMOS-compatible hybrid plasmonic waveguide for subwavelength light confinement and on-chip integration, *Opt. Express*, vol. 23, no. 4, pp. 206–208, 2011.
- [50] J. T. Kim, CMOS-compatible hybrid plasmonic slot waveguide for on-chip photonic circuits, *Opt. Express*, vol. 23, no. 20, pp. 1481–1483, Oct. 2011.
- [51] X. Zuo and Z. Sun, Low-loss plasmonic hybrid optical ridge waveguide on silicon-on-insulator substrate, *Opt. Express*, vol. 36, pp. 2946–2948, Aug. 2011.
- [52] J. Dintinger and O. J. F. Martin, Channel and wedge plasmon modes of metallic V-grooves with finite metal thickness, *Opt. Express*, vol. 17, pp. 2364–2374, 2009.

**Yusheng Bian** (S'11) received the B.S. degree in optical information science and technology from the Xi'an University of Technology, Shanxi, China, in 2006, and the M.S.E. degree in optical engineering from the Beijing Institute of Technology, Beijing, China, in 2008. He is currently working toward the Ph.D. degree in optical engineering in Beihang University, Beijing, China.

His current research interests include the design and fabrication of micro- and nanophotonic waveguides and devices. He has published more than 20 technical journal papers and conference talks.

Dr. Bian is a Student Member of the Lasers and Electro-Optics Society and the Optical Society of America.

**Zheng Zheng** (S'97 M'01) received the B.Eng. degree in electronic engineering from Tsinghua University, Beijing, China, in 1995, and the M.S.E.E. and Ph.D. degrees from Purdue University, West Lafayette, IN, in 1997 and 2000, respectively.

He was with the Optical Networking Group of Lucent Technologies, Holmdel, NJ, as a Member of Technical Staff, where he had conducted research on advanced optical fiber communications technologies. In December 2003, he joined Beihang University as a Full Professor. He has published more than 140 technical journal papers and conference talks. His current research interests include various areas in photonics and optical communications, such as novel photonic devices, plasmonics, ultrafast optics, and optical sensing.

Dr. Zheng received the Li Foundation Heritage Prize in 2004. He is a member of the Lasers and Electro-Optics Society and the Optical Society of America.

**Xin Zhao** received the B.E. and Ph.D. degrees from Beihang University, Beijing, China, in 2005 and 2011, respectively.

She is currently a Postdoctoral Researcher at Beihang University. Her current research interest includes the design of micro- and nanophotonic devices and ultrafast optics. She has authored more than 20 technical journal papers and conference talks.

**Yalin Su** received the B. Eng. degree in electronics engineering from the Beijing Institute of Technology, Beijing, China, in 2006. He is currently working toward the Ph.D. degree in physical electronics in Beihang University, Beijing.

His current research interests include optical communications and optical sensing and processing.

**Lei Liu** received the B.Eng. degree in electronics engineering from Shandong University, Jinan, China, in 2007. He is currently working toward the Ph.D. degree in physical electronics in Beihang University, Beijing, China.

His current research interests include ultrafast fiber lasers engineering and THz imaging.

**Jiansheng Liu** received the B.Sc. degree in optoelectronics physics from Shanxi University, Taiyuan, China, in 1985, and the Ph.D. degree in electrical engineering from Ulster University, Belfast, U.K., in 1995.

Since 1996, he has been with the School of Electronic and Information Engineering, Beihang University, Beijing, China, where he is currently a Professor and his research interests include photonic crystal fiber devices, nanophotonic device, fiber-optic sensors, biophotonic sensing, and nanophotonic structures for solar cell.

**Jinsong Zhu** received the B.A. degree in chemistry from Linfield College, McMinnville, OR, in 1993, and the Ph.D. degree from the University of Southern California, Los Angeles, in 1998.

After working at Lumera Corporation, Bothel, WA, as a Senior Engineer, and at Photon-X, Malvern, PA, as a Distinguished Scientist, where he had conducted research on organic nonlinear optical materials and rare earth photo luminescent materials, he joined the National Center for Nanoscience and Technology in June, 2005, as a Full Professor. His current research interests include various areas in biophotonics and optical communications, such as biochip sensing and ultrafast optical switch techniques. He has published more than 20 technical journal papers and presentation talks.

**Tao Zhou** received the B.S. degree in physics from Nanjing University, Nanjing, China, and the Ph.D. degree from the Max-Planck-Institut für Festkörperforschung, Stuttgart, Germany.

He joined NEC Laboratories and, later, Lucent Technologies-Bell Laboratories, NJ, where he was engaged in research on optical communications devices and technologies. He is an Assistant Professor with New Jersey Institute of Technology, Newark, where he is currently engaged in research on integrated optical circuits, photonic crystal, infrared optics, transition metal oxides, and Raman and infrared spectroscopy.